

Electrically driven light emission from hot single-walled carbon nanotubes at various temperatures and ambient pressures

Xinran Wang, Li Zhang, Yuerui Lu, and Hongjie Dai^{a)}

Department of Chemistry and Laboratory for Advanced Materials, Stanford University, Stanford, California 94305, USA

Y. K. Kato

PRESTO, Japan Science and Technology Agency, 4-1-8 Honcho Kawaguchi, Saitama 332-0012, Japan

Eric Pop

Intel Corporation, 2200 Mission College Boulevard, Santa Clara, California 95054, USA

(Received 1 September 2007; accepted 1 December 2007; published online 26 December 2007)

Electroluminescence of individual single-walled carbon nanotubes down to ~ 15 K is measured. We observe electrically driven light emission from suspended quasimetallic nanotubes in vacuum down to ~ 15 K and under different gas pressures at room temperature. Light emission is found to originate from hot electrons in the presence of electrically driven nonequilibrium optical phonons. Reduced light emission is observed in exponential manner as electron and optical phonon temperatures in the nanotube are lowered by lower ambient temperature or higher gas pressure. The results reveal over wide ambient conditions, light emission in a suspended tube is from thermally excited electron-hole recombination. © 2007 American Institute of Physics.

[DOI: 10.1063/1.2827281]

Single-walled carbon nanotubes (SWNTs) are one-dimensional (1D) materials with interesting optical and electro-optical properties due to the sharp peaks in the electronic density of states known as van Hove singularities.^{1,2} Photoluminescence and electroluminescence (EL) involving interband exciton recombination have been reported in semiconducting SWNTs (S-SWNTs).³⁻⁹ Earlier EL measurements on S-SWNTs attributed light emission from injected electron and hole recombination under bipolar operation.⁵ Recently, however, we observed strong thermally excited light emission in suspended quasimetallic (QM) SWNT transistors under unipolar operation.¹⁰ Optical phonon temperature (T_{op}) obtained from the high energy tail in visible light emission was in excellent agreement with the hot phonon model¹¹ and was used to reproduce the infrared spectra. These suggested that thermally generated carrier recombination was responsible for the light emission.¹⁰ On the other hand, other study⁶ on suspended metallic nanotube suggested that impact excitation could also lead to light emission, provided large enough electric field in the nanotube device. Both studies have shown exponential dependence of light emission intensity on bias voltage, yet how to distinguish the two mechanisms experimentally is still an open question.

In this work, we used two different methods to lower T_{op} in suspended SWNTs by decreasing ambient/metal contact temperature T_0 [Fig. 1(a)] and by increasing ambient gas pressure.¹² In all cases, we observed decreased electrical driven light emission intensity from QM-SWNTs as T_{op} was decreased. The hot optical phonon temperature was extracted within the framework of our nonequilibrium optical phonon model^{11,13} using an empirical SWNT thermal conductivity,¹⁴ and we found that light emission intensity was exponentially dependent on T_{op} down to 100 K ambient temperature. We

believe this universal dependence of light emission intensity on T_{op} is a clear signature of thermally excited light emission mechanism. The thermal light emission mechanism could be applicable to various hot SWNT devices, including suspended structures and nonsuspended ones operating at sufficiently high power dissipations.

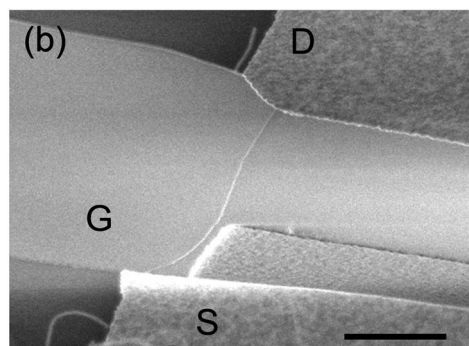
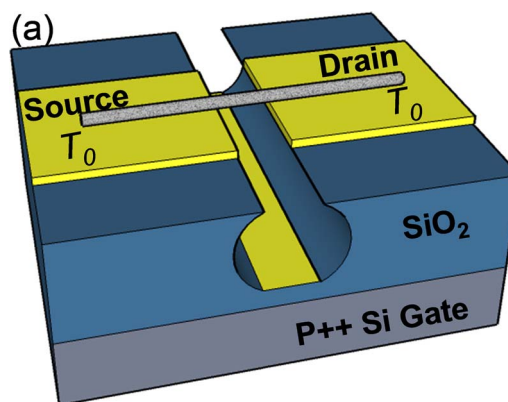


FIG. 1. (Color online) (a) Schematic drawing of our suspended SWNT devices with 10 nm W/20 nm Pt leads. (b) Scanning electron microscopy image of a typical suspended device over ~ 2 μm trench. Scale bar is 1 μm .

^{a)} Author to whom correspondence should be addressed. Electronic mail: hdai@stanford.edu.

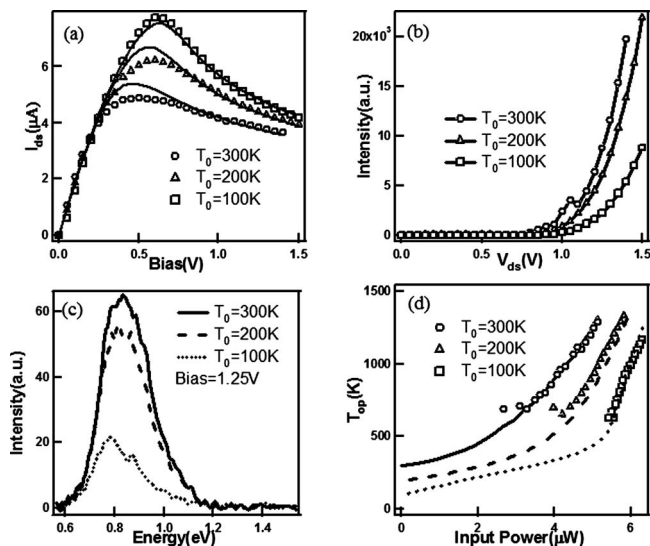


FIG. 2. Light emission data from a 2.5 μm long suspended quasimetallic device at various ambient temperatures in vacuum ($\sim 10^{-5}$ Torr). (a) Experimental data (symbols) and theoretical calculation (lines) of I - V characteristics under -15 V gate voltage. (b) Measured infrared light emission intensity vs bias. (c) Measured raw spectra at 1.25 V bias and -15 V gate bias. (d) Calculated optical phonon T_{op} (lines) temperatures vs input power from I - V curves. Symbols are $T_{\text{op}} \approx T_e$ from experimental light emission data and Eq. (2). The experimental light emissions stopped at certain input power because of our detection limit.

We used suspended CVD-grown QM-SWNTs that were 2–4 μm in length, bridging the W/Pt leads over a 1.5 μm deep trench and backgated by a heavily doped silicon substrate (Fig. 1). The fabrication processes were similar to those described elsewhere.¹⁰ All measurements were done inside a cryogenics probe station, where the heavily doped silicon backgate was both thermally and electrically well connected to the base plate of the probe station. Throughout this work, we treated that the contact temperature T_0 was equal to ambient temperature (down to ~ 15 K). We used specially designed optical fiber coupled with an objective lens (numerical aperture of approximately ~ 0.4 , working distance ~ 1 mm) to collect the light and sent it into spectrometer and detector.¹² SEM images were taken after all the measurements to ensure single nanotube connection and to get the length information.

We then investigated the ambient temperature dependence of light emission intensity under a constant vacuum of $\sim 10^{-5}$ Torr. At $T_0 \sim 300$ K, the current through nanotubes together with light emission intensity were recorded as a function of bias under a fixed gate voltage of -15 V [Figs. 2(a) and 2(b)]. Due to insufficient heat dissipation in the suspended nanotubes and hot optical phonon population,¹¹ the I - V characteristics exhibited negative differential conductance (NDC) region beyond ~ 0.5 V, where light emission grew exponentially with bias [Fig. 2(b)]. The same measurements were repeated at $T_0 \sim 200, 100,$ and 15 K [Fig. 2, 15 K data not shown]. As T_0 went down, current significantly increased in the NDC region at a given bias, while light emission intensity became much lower. This observation which was qualitatively explained by that lower T_0 gave lower T_{op} in the SWNTs, resulting in lower thermal electron occupation at first van Hove singularity (thus lower light emission intensity) and reduced electron-phonon scattering (thus higher current).

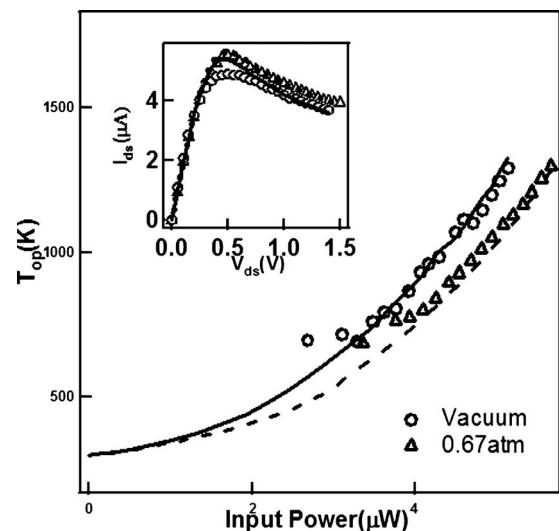


FIG. 3. Calculated T_{op} (lines) vs input power for the same device as Fig. 2 at $T_0 = 300$ K, in vacuum and 0.67 atm argon, respectively. Symbols are $T_{\text{op}} \approx T_e$ from experimental light emission data and Eq. (2), with the same fitting parameter I_0 as in Fig. 2. The inset shows the experimental I - V curves (symbols) and fits (lines).

We also varied ambient gas pressure and measured light emission of suspended SWNTs at room temperature in 0.67 atm of argon and compared with the result in vacuum (Fig. 3). In argon, current was slightly higher than in vacuum due to better heat dissipation through optical phonon relaxation by the gas molecules surrounding the nanotube.¹² Therefore, gas molecules acted as an effective “cooler” for the nanotube. As a result, the light emission intensity was slightly decreased in argon ambient (data not shown), as we would expect in our thermal picture.

In order to study light emission intensity quantitatively, we extracted the hot phonon temperature as a function of power dissipation by fitting the I - V characteristics^{11,13,14} (see supplementary material¹⁵ for calculation details). We can use two fitting parameters: the hot-phonon parameter α defined as $T_{\text{op}} = T_{\text{ac}} + \alpha(T_{\text{ac}} - T_0)$ and contact thermal resistance R_{cth} to fit experimental I - V curves under all conditions (Table I in supplementary material¹⁵ shows the parameters used in simulation). We emphasize that the inclusion of R_{cth} and contact heating effect is necessary to reproduce the experimental curves, which has not been observed experimentally and modeled theoretically. In Figs. 2(a) and 3 inset, we show the calculated I - V curves (lines), which are in very good agreement with experimental data. The extracted optical phonon temperatures at various conditions are also plotted in Figs. 2(d) and 3 (lines).

In earlier work, we had proposed that the intensity of thermal light emission should be exponentially dependent on optical phonon temperature as¹⁰

$$I = I_0 \exp\left(-\frac{E}{k_B T_{\text{op}}}\right), \quad (1)$$

with $T_{\text{op}} \approx T_e$ obtained from the blackbodylike tail of visible light emission and I_0 as a fitting parameter (I_0 is the saturation intensity at infinite temperature, proportional to the transition probability). We invert Eq. (1) as

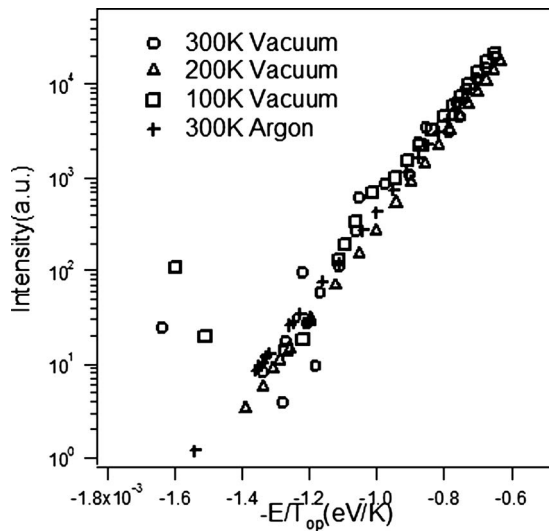


FIG. 4. Light emission intensity vs $-E/k_B T_{op}$ for all cases in Figs. 2 and 3.

$$T_{op} = \frac{-E}{k_B \log(I/I_0)}. \quad (2)$$

By reading E from the peak position in the spectra [Fig. 2(c)] and selecting a proper temperature independent I_0 , we could get the optical phonon temperature from the experimental light emission intensity I . It turned out that a single value of I_0 could reproduce the calculated T_{op} from I - V data and hot phonon model for all four cases studied in this work [100–300 K in vacuum and 300 K in argon, shown in Figs. 2(d) and 3]. The agreement between the T_{op} indicates that Eq. (2) is the correct model to understand the light emission in our devices. The relation between I and T_{op} is rather general in various ambient conditions. In Fig. 4, we plot the experimental I versus $-E/k_B T_{op}$ in log scale for all the four cases, and they indeed overlap very well in an exponential manner. This simple scaling is a strong evidence that the light emission from our devices is from thermally excited electron-hole recombination.

We noted a recent theoretical work¹⁶ that considered the effect of optical phonon temperature and predicted

$$I = I_0 \exp\left(-\frac{E}{\sqrt{(k_B T_{op})^2 + (eF\lambda_{op})^2}}\right), \quad (3)$$

where F is the electric field in the SWNTs, λ_{op} is optical phonon mean free path, and E is the threshold energy. This equation points out two competing mechanisms that lead to light emission in SWNT devices: thermal effect and impact excitation of high energy electrons due to high electric field. In our devices, $T_{op} \sim 1000$ K, while $\lambda_{op} \sim 15$ nm in the NDC region at room temperature,¹¹ and $F \sim 0.5$ MV/m, so the thermal term ($k_B T_{op} \sim 0.086$ eV) is dominant over the impact excitation term ($eF\lambda_{op} \sim 0.0075$ eV). Therefore, we see the

scaling of light emission intensity with T_{op} , indicating it is in thermal nature. This condition should hold in the relatively long suspended nanotube devices ($L \geq 1 \mu\text{m}$), but in the short devices, the electric field could be high enough for the impact excitation term to be comparable to the thermal term. The same situation could also occur in nonsuspended devices since T_{op} could be much lower than 1000 K.¹⁷

In summary, we studied the ambient temperature and pressure dependence of electrically driven infrared light emission from suspended QM SWNTs. We found that the intensity was exponentially dependent on the optical phonon temperature T_{op} in all T_0 down to 100 K as well as in argon ambient, suggesting that the light emission originates from the recombination of thermally excited electrons and holes. This universal dependence could be used as one of the signatures of thermal light emission. We discussed the two possible light emission mechanisms in light of recent theoretical calculation, and believed that the thermal mechanism should be the dominant mechanism in relatively long suspended SWNT devices as in our case. The thermal mechanism should be considered in future nanotube electroluminescence research and applications.

¹M. S. Dresselhaus and H. Dai, MRS Bull. **29**, 237 (2004).

²R. Saito, M. Fujita, G. Dresselhaus, and M. S. Dresselhaus, Phys. Rev. B **46**, 1804 (1992).

³M. J. O'Connell, S. M. Bachilo, C. B. Huffman, V. C. Moore, M. S. Strano, E. H. Haroz, K. L. Rialon, W. H. Noon, C. Kittrell, J. Ma, R. H. Hauge, R. Bruce Weisman, and R. E. Smalley, Science **297**, 593 (2002).

⁴J. Lefebvre, Y. Homma, and P. Finnie, Phys. Rev. Lett. **90**, 217401 (2003).

⁵M. Freitag, J. Chen, J. Tersoff, J. C. Tsang, Q. Fu, J. Liu, and P. Avouris, Phys. Rev. Lett. **93**, 076803 (2004).

⁶J. Chen, V. Perebeinos, M. Freitag, J. Tsang, Q. Fu, J. Liu, and P. Avouris, Science **310**, 1171 (2005).

⁷L. Marty, E. Adam, L. Albert, R. Doyon, D. Menard, and R. Martel, Phys. Rev. Lett. **96**, 136803 (2006).

⁸J. A. Misewich, R. Martel, Ph. Avouris, J. C. Tsang, S. Heinze, and J. Tersoff, Science **300**, 783 (2003).

⁹F. Wang, G. Dukovic, L. E. Brus, and T. F. Heinz, Science **308**, 838 (2005).

¹⁰D. Mann, Y. K. Kato, A. Kinkhabwala, E. Pop, J. Cao, X. Wang, L. Zhang, Q. Wang, J. Guo, and H. Dai, Nat. Nanotechnol. **2**, 33 (2007).

¹¹E. Pop, D. Mann, J. Cao, Q. Wang, K. Goodson, and H. Dai, Phys. Rev. Lett. **95**, 155505 (2005).

¹²D. Mann, E. Pop, J. Cao, Q. Wang, K. Goodson, and H. Dai, J. Phys. Chem. B **110**, 1502 (2006).

¹³E. Pop, D. Mann, K. Goodson, and H. Dai, J. Appl. Phys. **101**, 093710 (2007).

¹⁴E. Pop, D. Mann, Q. Wang, K. Goodson, and H. Dai, Nano Lett. **6**, 96 (2006).

¹⁵See EPAPS Document No. E-APPLAB-91-075752 for the calculation details used in the paper and the parameters in calculation. This document can be reached through a direct link in the online article's HTML reference section or through the EPAPS homepage (<http://www.aip.org/pubservs/epaps.html>).

¹⁶V. Perebeinos and P. Avouris, Phys. Rev. B **74**, 121410(R) (2006).

¹⁷E. Pop, D. Mann, J. Reifenberg, K. Goodson, and H. Dai, Tech. Dig. - Int. Electron Devices Meet. **2005**, 253.